Original article

Dual-site beta tACS over rIFG and M1 enhances response inhibition: A parallel multiple control and replication study

Qiujian Meng [a],[¶], Ying Zhu [a],[¶], Ye Yuan [a], Rui Ni [a],[b], Li Yang [a], Jiafang Liu [a], Junjie Bu [a],[*]

[a] Department of Intelligent Medical Engineering, School of Biomedical Engineering, Anhui Medical University, Hefei, China
[b] Department of Life Sciences, Imperial College London, London, United Kingdom

ARTICLE INFO

ABSTRACT

Response inhibition is a core component of cognitive control. Past electrophysiology and neuroimaging studies have identified beta oscillations and inhibitory control cortical regions correlated with response inhibition, including the right inferior frontal gyrus (rIFG) and primary motor cortex (M1). Hence, increasing beta activity in multiple brain regions is a potential way to enhance response inhibition. Here, a novel dual-site transcranial alternating current stimulation (tACS) method was used to modulate beta activity over the rIFG-M1 network in a sample of 115 (excluding 2 participants) with multiple control groups and a replicated experimental design. In Experiment 1, 70 healthy participants were randomly assigned to three dual-site beta-tACS groups, including in-phase, anti-phase or sham stimulation. During and after stimulation, participants were required to complete the stop-signal task, and electroencephalography (EEG) was collected before and after stimulation. The Barratt Impulsiveness Scale was completed before the experiment to evaluate participants' impulsiveness. In addition, we conducted an active control experiment with a sample size of 20 to exclude the potential effects of the dual-site tACS "return" electrode. To validate the behavioural findings of Experiment 1, 25 healthy participants took part in Experiment 2 and were randomized into two groups, including in-phase and sham stimulation groups. We found that compared to the sham group, in-phase but not anti-phase beta-tACS significantly improved both response inhibition performance and beta synchronization of the inhibitory control network in Experiment 1. Furthermore, the increased beta synchronization was correlated with enhanced response inhibition. In an independent sample of Experiment 2, the enhanced response inhibition performance observed in the in-phase group was replicated. After combining the data from the above two experiments, the time dynamics analysis revealed that the in-phase beta-tACS effect occurred in the post-stimulation period but not the stimulation period. The state-dependence analysis showed that individuals with poorer baseline response inhibition or higher attentional impulsiveness had greater improvement in response inhibition for the in-phase group. These findings strongly support that response inhibition in healthy adults can be improved by in-phase dual-site beta-tACS of the rIFG-M1 network, and provide a new potential treatment targets of synchronized cortical network activity for patients with clinically deficient response inhibition.

Introduction

Response inhibition is the process of terminating behaviours or plans that no longer meet the requirements of the current environment, allowing people to engage in flexible, goal-directed behaviours in response to the changed environment (G. D. J. A. p. Logan, 1985). Response inhibition is an essential component of cognitive control (Ridderinkhof, Van Den Wildenberg, Segalowitz, Carter, & Cognition, 2004), and its neural mechanisms have been a focus of neuroscience

research. A growing number of neuroimaging studies have shown that response inhibition involves cortical brain regions, including the right inferior frontal gyrus (rIFG) and primary motor cortex (M1) (Boehler, Appelbaum, Krebs, Hopf, & Woldorff, 2010; Depue, Orr, Smolker, Naaz, & Banich, 2016; Rae, Hughes, Anderson, & Rowe, 2015). The rIFG has been considered the core component of the inhibitory control network, acting as a brake on response tendencies(Aron, Robbins, & Poldrack, 2014). The latest study found that M1 interspersed with integrated regions of the somato-cognitive action network is associated with response

inhibition (Gordon et al., 2023). Additionally, electrophysiology studies have revealed that beta oscillatory (13–30 Hz) activity is critical for response inhibition in regulating brain network communication (Swann et al., 2009; Wagner, Wessel, Ghahremani, & Aron, 2018). Thus, modulation of beta activity between the rIFG and M1 is a potential way to enhance response inhibition.

At present, non-invasive brain stimulation (NIBS) studies have mainly focused on the effects of single brain regions on response inhibition (Hsu et al., 2011; Jacobson, Javitt, & Lavidor, 2011; Kwon et al., 2013; Kwon & Kwon, 2013; Stramaccia et al., 2015). Notably, the results of previous NIBS studies were at the center of controversy, in which some studies failed to improve response inhibition (Dambacher et al., 2015; Kwon & Kwon, 2013; Thunberg, Messel, Raud, & Huster, 2020). This discrepancy across NIBS studies may be related to not considering communications in inhibitory control networks. Past evidences have suggested that intercommunication of brain regions relies on the oscillatory synchronization of neuronal activity (Fries, 2015; Parkin, Hellyer, Leech, & Hampshire, 2015). Studies that simultaneously measured electroencephalography (EEG) activity during the execution of the response inhibition task found increased beta activity of the rIFG and M1 during successful response inhibition, suggesting functional coupling between the M1 and rIFG in the beta band during response inhibition. In addition, transcranial magnetic stimulation pulses were applied to the rIFG during the response inhibition task while M1 motor evoked potentials were measured, and motor evoked potentials peaks consistent with 20 Hz were found, indicating functional coupling in the beta frequency band between the M1 and rIFG during response inhibition (Picazio et al., 2014). Therefore, promoting beta synchronization of the rIFG-M1 network by NIBS may enhance response inhibition.

Recently, dual-site transcranial alternating current stimulation (tACS), as a novel NIBS where two stimulation electrodes are placed in two different target cortical brain regions and a third "return" electrode is placed in an irrelevant region, has been used to modulate endogenous oscillations between brain regions and thus modulate motor or cognitive function (Helfrich et al., 2014; Polanía, Nitsche, Korman, Batsikadze, & Paulus, 2012; Violante et al., 2017). The modulatory effects of dual-site tACS have been shown to be phase-dependent. Simultaneous recording of EEG activity during the application of dual-site tACS showed that in-phase (IP) dual-site tACS (synchronization condition, 0° phase offset) enhanced frequency-specific phase coupling of electrophysiological signals between stimulation sites and strengthened cognitive function, whereas anti-phase (AP) dual-site tACS (desynchronization condition, 180° phase offset) had no such effects. Crucially, several studies have used dual-site tACS to demonstrate the causal relationship between inter-regional oscillatory synchronization and improved working memory performance. By applying dual-site theta tACS in the fronto-parietal network, they found that IP tACS significantly improved working memory compared with AP tACS and sham (Polanía et al., 2012; Violante et al., 2017). Thus, dual-site tACS provides a non-invasive and potential tool for modulating the beta activity of the rIFG-M1 network and improving response inhibition.

The study had a sample size of 115 (excluding 2 participants), with a randomized, multiple control group and replicated experimental design. Dual-site beta-tACS (20 Hz) was used to modulate beta activity in the rIFG-M1 network and to investigate the effects on response inhibition. In Experiment 1, 70 healthy participants were randomly assigned to three dual-site beta-tACS groups, including IP, AP or sham stimulation. Additionally, the stimulation site in the left supraorbital area control experiment (lSOA control, $n = 20$) was used to exclude the potential effects of the dual-site tACS "return" electrode. To test the replicability of the behavioural effects induced by dual-site tACS, we performed an independent sample of Experiment 2 ($n = 25$) in which healthy participants were randomly assigned to IP or sham stimulation groups. All participants completed the stop-signal task during and after stimulation, and open-eyes resting-state EEG were collected before and after stimulation. The Barratt Impulsiveness Scale (BIS11) assesses participants'

impulsiveness. The weighted phase lag index (WPLI) between brain regions was calculated to assess functional connectivity. We found that 1) participants in IP but not AP stimulation showed increased beta synchronization of the inhibitory control network indexed by beta-WPLI and enhanced response inhibition compared to sham. In addition, the increase in beta-WPLI was correlated with the improvement in response inhibition; 2) behavioural improvement by IP rIFG-M1 stimulation was replicated in an independent sample of Experiment 2; 3) IP dual-site tACS behavioural effect was demonstrated in the post-stimulation period; and 4) the behavioural improvement was state-dependent on baseline cognitive control.

Materials and methods

Participants

A total of 115 healthy college students were recruited for this study, with 2 participants voluntarily withdrawing before the completion of the experiment (from Experiment 1). Data from the remaining 113 participants were included in the analysis (Experiment 1, $n = 88$; Experiment 2, $n = 25$) (Fig. 1). Inclusion criteria included age of 18 years or older; normal or corrected-to-normal vision; no metal implants or implanted electronic devices in the head; and no history of neurological disease, traumatic brain injury, substance abuse, or family history of epilepsy. Experiment 1 consisted of an IP dual-site beta-tACS over rIFG-M1 network stimulation group (rIFG-M1 IP, $n = 25$), an AP dual-site beta-tACS over rIFG-M1 network stimulation group (rIFG-M1 AP, $n = 24$), a sham stimulation group (sham, $n = 20$), and lSOA control ($n = 19$). Experiment 2 included rIFG-M1 IP ($n = 15$) and sham groups ($n = 10$). All study procedures were approved by the Ethics Committee. Participants provided informed consent before participating in the study.

In Experiment 1, we performed a post hoc analysis of statistical power based on a two-way mixed-design ANOVA (e.g., rIFG-M1 and sham) with Cohen's F of 0.25 and a sample size of 45 participants sufficient to achieve 91% statistical power at the $p = 0.05$ level of significance.

In Experiment 2, we calculated the necessary sample size based on an a priori analysis of the main results of Experiment 1. Based on the two-way mixed-design ANOVA of Experiment 1 (e.g., rIFG-M1 and sham), Cohen's F was 0.39, and the sample size of 20 participants was sufficient to achieve a statistical validity of 91% at the $p = 0.05$ level of significance.

Experimental procedure

We used a randomized, multiple control group and double-blind experimental design. One researcher was responsible for data collection and was unaware of the stimulation conditions. The other researcher was responsible for setting up the tACS intervention (active or sham) and was not involved in any data collection. Participants' basic demographic information, including age, sex and education, was recorded before the start of the experiment. Participants completed the BIS11, which assesses impulsiveness on three dimensions: Attentional Impulsiveness (AI), Motor Impulsiveness (MI), and Non-Planning Impulsiveness (NPI), with higher ratings indicating greater impulsiveness. The experiment included the following procedures (Fig. 2a): 1) participants sat comfortably on the sofa and remained relaxed. They were asked to look at the fixation point in the center of the computer screen and recorded a 5 min open-eyes resting state electroencephalography (EEG); 2) they completed SST combined with 20 min of tACS. Participants were asked to assess their feelings before and after the tACS intervention, including concentration level, emotional peace, fatigue level, and visual perceptiveness, pre- and poststimulation. In addition, participants rated their subjective experience of any tACS side effects, including itch, headache, burning sensation, warmth, tingling sensation,
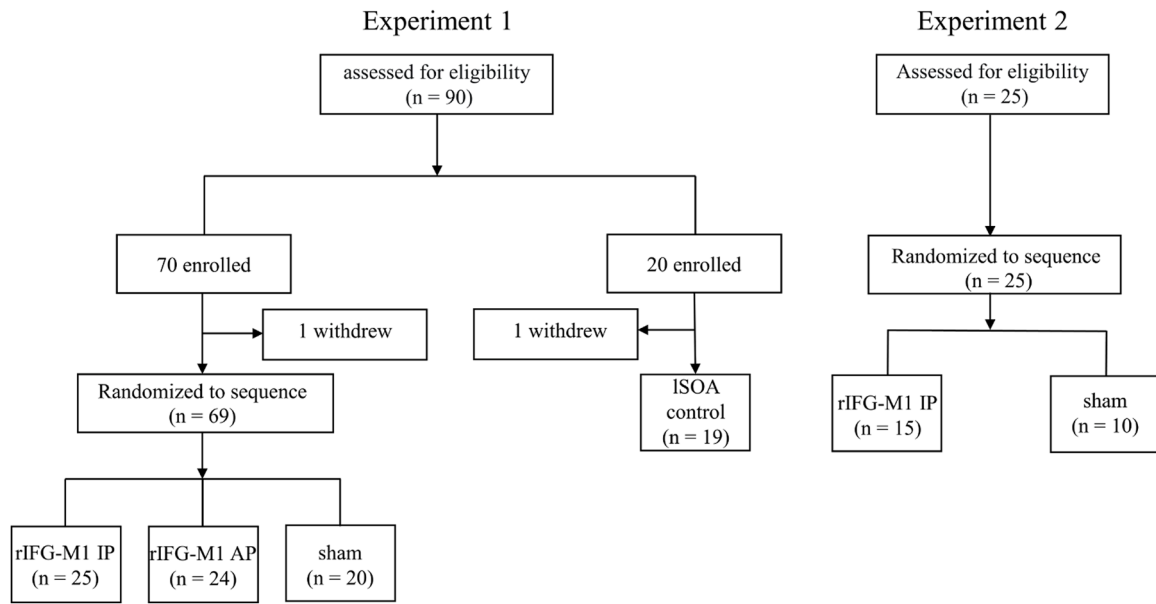
Fig. 1. Schematic diagram of the participants.
rIFG = right inferior frontal gyrus, M1 = primary motor cortex, lSOA = left supraorbital area, IP = in-phase, AP = anti-phase.
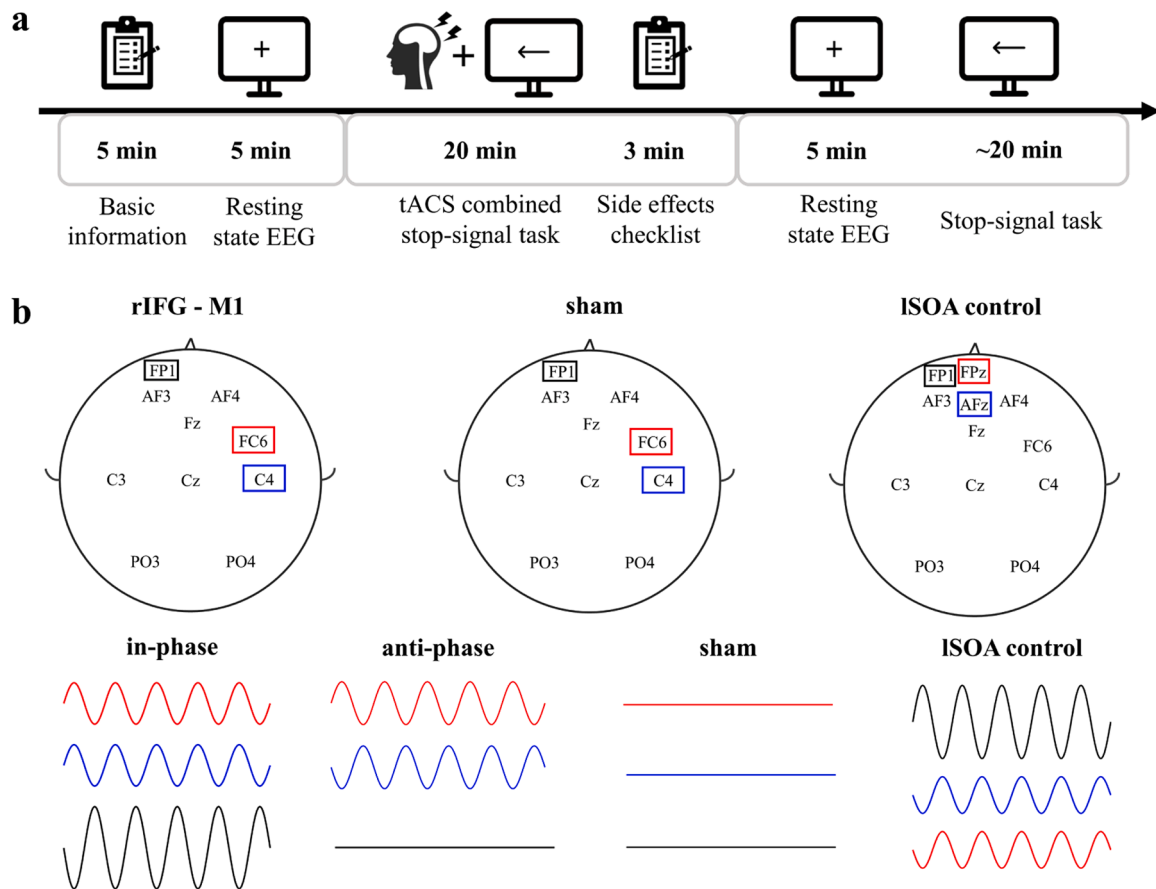
Fig. 2. Experimental protocol and tACS parameters.
(a) Schematic illustration of the experimental procedure. **(b)** tACS electrode setup. tACS = transcranial alternating current stimulation, rIFG = right inferior frontal gyrus, M1 = primary motor cortex, IP = in-phase, AP = anti-phase, lSOA = left supraorbital area.

metallic taste, fatigue, dizziness, nausea, phosphene, and others, on a numeric scale (0–4, with 0 indicating none and 4 indicating strong); 3) resting EEG signals were recorded for 5 min with participants' eyes open, and 4) participants completed the SST test. At the end of the experiment, the researchers and each participant were asked if they could guess the type of stimulation performed, including real

stimulation, placebo stimulation, or uncertain. All participants were randomly assigned to each experimental group. Experiment 2 had the same experimental procedure as Experiment 1. Analysis of the post experimental questionnaire showed no significant difference between the stimulated groups and sham group in terms of both pre- and post-stimulation feelings (Supplementary Fig 1a) and tACS side effects (Supplementary Fig 1b), and the researchers and participants were unable to distinguish the types of stimulation (Supplementary Fig 1c).

Stop-signal task

The SST was programmed in MATLAB (R2019b, MathWorks, Natick, MA) using Psychtoolbox3.0. Go trials (67% of total trials) were initiated by a fixation icon presented on a white computer screen for 500 ms. A black arrow pointing left or right appeared behind the fixation icon for 200 ms. Participants were asked to judge the direction of the arrows as accurately and quickly as possible by pressing a key with their left ("F" for left) and right ("J" for right) index finger. Stop trials (33% of total trials) initially appeared like go trials, with a red dot appearing after a variable stop-signal delay (SSD), prompting participants to inhibit the response. The initial value of SSD was 100 ms. SSD increased by 50 ms after each successful stop trial and decreased by 50 ms after an unsuccessful stop trial, thereby ensuring a successful stop accuracy of nearly 50%. Participants completed practice blocks of 96 trials before the first test began to ensure that they could understand and adhere to the task instructions. Two blocks of SST were administered for each assessment. Each block contained 192 trials.

The response inhibition efficiency of participants was estimated by calculating the SSRT (Verbruggen et al., 2019). Longer SSRT was associated with worse response inhibition (G. D. J. T. Q. J. o. E. P. Logan, 2015). In addition to SSRT, we evaluated go reaction time (go RT), failed stop reaction time (failed stop RT), go accuracy, stop accuracy and SSD. All behavioural analyses were performed with custom MATLAB scripts and in R Studio's SSRTcalc package 0.3.3. Based on previous practice (Congdon et al., 2012; Verbruggen et al., 2019), the results of mean failed stop RT < mean Go RT and stop accuracy below 25% or above 75% were excluded. According to the latest consensus recommendation (Verbruggen et al., 2019), SSRT was calculated using the integral method with replacement of go omissions. Data from 113 participants in Experiments 1 and 2 were included in the analysis. Visual inspection of the QQ plots showed that the SSRT data were normally distributed.

tACS

In Experiments 1 and 2, tACS was delivered using a Starstim transcranial alternating current stimulator and Ag/AgCl circular electrodes with an area of 3.14 cm^2. The electrode position was determined by the international 10–20 system. The stimulation electrodes were in FC6 (Hogeveen et al., 2016) and C4 (Kwon & Kwon, 2013) for the rIFG-M1 network. Referring to previous related studies (Kwon et al., 2013; Stramaccia et al., 2015), the "return" electrode was placed on the left supraorbital region in all stimulation conditions (Fig. 2b). The 20 Hz (Enz, Ruddy, Rueda-Delgado, & Whelan, 2021; Leunissen et al., 2022; Wessel, 2020)sinusoidal currents were applied with 1 mA peak-to-peak to both stimulation sites for 20 min at a 0° phase offset (IP) or 180° phase offset (AP) tACS conditions. There was a 10 s ramp-up/down of currents at the beginning and end of stimulation. For the sham stimulation with a gradual increase and then a gradual decrease over a 40 s window at the beginning and end of the stimulation period and none of the currents at the other times. The primary purpose of lSOA control was to rule out that the behavioural changes in Experiment 1 were due to the stimulation of the "return" electrode, so the stimulation electrode was located on the left supraorbital area. The "return" electrodes were located on AFz and Fpz (Fig. 2b). The stimulation duration of a sinusoidal current at 20 Hz peak-to-peak of 2 mA was 20 min, with a 10 s ramp-up/down of the currents at the beginning and end of the stimulation. The impedance remained below 10 kΩ in all conditions. The intervention was well tolerated by all participants.

The electric field distribution (Supplementary Fig 2) generated by dual-site tACS was calculated using SimNIBS v3.2.6, enabling finite element methods (Thielscher, Antunes, & Saturnino, 2015). The given template header model of the sample dataset (ernie. msh) was utilized. Electrodes with a 1 cm radius were placed in each target region (2 mm thickness for the electrode layer and 3 mm thickness for the gel). In the IP tACS condition, each stimulating electrode current was +0.5 mA, and the "return" electrode current was −1 mA. In the case of the AP tACS condition, the two stimulating electrode currents cancelled each other, and the two stimulating electrode currents were 0.5 mA and −0.5 mA. For lSOA control, the stimulating electrode current was 1 mA, and each "return" electrode current was −0.5 mA. By dividing the current density vector by the grey matter conductivity, the normal component of the electrical field on the grey matter can be calculated.

EEG recording and analysis

EEG data were collected with a Starstim 8-channel system (Neuroelectrics, Spain) with a sampling rate of 500 Hz. Channels were distributed over AF3, AF4, C3, C4, Fz, Cz, PO3, and PO4. For the reference (CMS) and ground (DLR), we use an ear clip with dual CMS-DLR electrodes on the right earlobe. Impedance was required to stay below 10 kΩ. EEG was recorded pre- and post-tACS for 5 min each time.

EEG pre-processing was performed using the eeglab toolbox in MATLAB. A 1–80 Hz bandpass filter and 50 Hz notch filtering were applied for raw data. Blinking, breathing, and heart artifacts were manually removed. Data were segmented into 2 s epochs with thresholds below −100 μV or above 100 μV removed and were averaged over all epochs. Data from 6 participants from Experiment 1 (rIFG-M1IP: 2 participants, sham: 1 participant) and Experiment 2 (sham: 3 participants) were excluded due to excessive artifacts.

Functional connectivity was assessed by calculating the weighted phase lag index (WPLI) for each frequency (delta: 1–4 Hz, theta: 4–7 Hz, alpha 7–13 Hz, beta: 13–30 Hz), which was implemented in MATLAB and referred to Vinck et al. (2011). The WPLI is insensitive to additional, uncorrelated noise sources and thus was used to examine the phase synchronization between two time series signals, expressed as the absolute value of the imaginary component of the crossover spectrum. The WPLI was calculated for channel-pairs with C4 (e.g., C4-PO4) as the target.

Statistical analysis

Statistical analyses were performed with SPSS 23.0 (IBM, USA). One-way ANOVA was used to evaluate age, education, BIS11 rating, BIS11 subscales, and baseline SSRT for all stimulation groups. A two-sided chi-square test was used to analyse sex and stimulation condition blindness. To explore the effect of tACS on SSRT and WPLI, we used two-way mixed-design ANOVA using group (e.g., rIFG-M1 IP, sham, and rIFG-M1 AP) as a between-subjects factor and time (e.g., during stimulation and poststimulation) as a within-subjects factor. Multivariate ANOVA (MANOVA) was utilized to assess the side effects caused by tACS. Behavioural differences during and after the stimulation within each group were calculated using paired t tests. Two-sample t-tests were used to compare the differences between groups of behavioural data blocks. Pearson correlation analysis was used to determine the correlation between SSRT change and WPLI change, as well as between BIS11 ratings and SSRT performance. For all tests, a two-tailed $p < 0.05$ was regarded as significant.

Results

Basic demographic characteristics of the stimulation groups

In Experiment 1, we compared the basic demographic characteristics of the three stimulation groups. Age, sex, education, BIS11 rating, and its subscales did not differ significantly among the three stimulation groups (Table 1). Similarly, there were no differences in the basic information between the two stimulation groups in Experiment 2 (Table 1).

IP rIFG-M1 stimulation improved SST performance

We first investigated how dual-site beta-tACS affected SST performance on stop-signal reaction time (SSRT), a measure of response inhibition that is frequently employed (Alderson, Rapport, & Kofler, 2007), and shorter SSRT is associated with better response inhibition. In Experiment 1, a two-way mixed-design analysis of variance (ANOVA) was performed to evaluate SSRT, with group (rIFG-M1 IP, sham, and rIFG-M1 AP) as a between-subjects factor and time (during-stimulation and post-stimulation) as a within-subjects factor. The results yielded a significant group × time interaction ($F_{2,66} = 4.49$, $p = 0.02$, $\eta_p^2 = 0.12$; Fig. 3a), and the SSRT collected during stimulation did not significantly differ among the three groups ($F_{2,66} = 0.33$, $p = 0.72$; one-way ANOVA). Further analysis revealed that rIFG-M1 IP induced a significant SSRT reduction compared to sham ($F_{1,43} = 6.66$, $p = 0.01$, $\eta_p^2 = 0.13$; Fig. 3a) and rIFG-M1 AP ($F_{1,47} = 6.81$, $p = 0.01$, $\eta_p^2 = 0.13$; Fig. 3a), whereas rIFG-M1 AP induced no significant difference in SSRT compared to sham. Fig. 3b shows the changes in SSRT for each individual for all stimulation groups. Apart from SSRT, other SST measures are shown in Supplementary Table 1; of these measures, stop accuracy and stop-signal delay (SSD) were significantly higher in the rIFG-M1 IP group compared to the sham group (Supplementary Figs 3 g and 3i).

Considering that the targets of our dual-site tACS were all in the right hemisphere, we further intended to observe whether there was a lateralization effect of the stimulation. We found no significant difference between the right- and left-handed performance of the rIFG-M1 IP, sham and rIFG-M1 AP groups (two-way mixed design ANOVA), ruling out a lateralization effect of the stimulation.

IP rIFG-M1 stimulation enhanced beta synchronization

In Experiment 1, two-way mixed design ANOVAs were performed on the WPLIs across channel pairs activated in the electric field simulation that were involved in the inhibitory control network (with C4 as the seed and connections to Cz, AF4, and PO4, respectively) in various bands (delta, theta, alpha and beta) of resting-state EEG with group (rIFG-M1 IP, sham) as a between-subjects factor and time (pre-stimulation, post-stimulation) as a within-subjects factor. A significant group × time interaction was observed only in the beta-WPLI of the C4-PO4 pair in the rIFG-M1 IP and sham groups ($F_{1,40} = 6.56$, $p = 0.01$, $\eta_p^2 = 0.14$; Fig. 4a), but not for delta, theta and alpha WPLI, indicating the frequency specificity of IP rIFG-M1 stimulation. Additionally, there were no significant differences observed between the C4-PO4 beta-WPLI of the rIFG-M1 AP and the sham groups (Fig. 4b). Crucially, in the rIFG-M1 IP group, a significant correlation was identified between the enhancement of C4-PO4 beta-WPLI and the reduction in SSRT scores ($r = -0.46$, $p = 0.03$, Pearson correlation; Fig. 4c). However, no such correlation was observed in the rIFG-M1 AP and sham groups.

Furthermore, we seeded electrode AF3 near the return electrode and analyzed its connectivity with C4 to exclude the potential influence of the "return" electrode effect on the primary outcome of the experiment. There was no significant group × time interaction (two-way mixed design ANOVA) between AF3-C4 beta-WPLI in the rIFG-M1 IP and sham groups, precluding the impact of the stimulation effect of the "return" electrode on beta synchronization or desynchronization.

Control analysis

To exclude the behavioural effect of the dual-site tACS "return" electrode, we performed a "return" electrode control experiment. Age, sex, and education did not differ significantly between the lSOA control and sham groups (all $p > 0.05$). A two-way mixed design ANOVA was conducted on the change in SSRT with group (lSOA control, sham) as a between-subjects factor and time (during-stimulation, post-stimulation) as a within-subjects factor, and there was no significant group × time interaction ($F_{1,37} = 0.87$, $p = 0.36$, $\eta_p^2 = 0.02$; Fig. 5a), indicating that the stimulation effect at the "return" electrode had no effect on the behavioural outcome.

Replication of behavioural findings for IP rIFG-M1 stimulation

In Experiment 2, we sought to replicate the behavioural findings in a new cohort of participants. A two-way mixed-design ANOVA using group (rIFG-M1 IP and sham) as a between-subjects factor and time (during-stimulation and post-stimulation) as a within-subjects factor on the SSRT. Compared to the sham group, the rIFG-M1 IP group showed more SSRT reduction ($F_{1,23} = 4.58$, $p = 0.04$, $\eta_p^2 = 0.17$; Fig. 6a). The during-stimulation SSRT did not significantly differ between the two groups ($t_{23} = 1.70$, $p = 0.10$, Cohen's $d = 0.71$; two-sample t-test). Fig. 6b shows the changes in SSRT for each individual in the two stimulation groups. Other SST measures of Experiment 2 are shown in Supplementary Table 1, and no measures had a difference compared to the sham group (Supplementary Fig 3f).

To summarize, we found that IP rIFG-M1 stimulation effectively improved SST performance, which was further replicated in an independent sample.

Time dynamics of the improvements in SST

Next, we examined the evolution and dynamics of behaviour during- and post-stimulation periods by sorting the data into four blocks in the combined Experiments 1 and 2. The SSRT of block1 did not differ significantly between the rIFG-M1 IP and sham groups ($t_{68} = 1.68$, $p = 0.10$, Cohen's $d = 0.41$; two-sample t-test). Thus, we considered the SSRT in block 1 as the baseline and examined the significant differences

Table 1
Basic demographic characteristics of the stimulation groups.

Experiment 1				
	rIFG-M1 IP, $n = 25$	sham, $n = 20$	rIFG-M1 AP, $n = 24$	P
Age (years)	21.76 (1.76)	21.55 (1.28)	21.42 (1.21)	0.71[a]
Sex (male/female)	18/7	14/6	16/8	0.92[b]
Education (years)	15.84 (1.68)	15.00 (1.30)	15.63 (1.13)	0.13[a]
BIS11	57.28 (7.67)	55.15 (7.03)	59.29 (6.98)	0.18[a]
AI	12.96 (2.23)	13.20 (2.31)	13.88 (2.40)	0.37[a]
MI	18.32 (3.28)	17.40 (2.98)	18.29 (3.16)	0.56[a]
NPI	26.00 (4.43)	24.55 (4.56)	27.13 (3.57)	0.14[a]
Experiment 2				
	rIFG-M1 IP, $n = 15$	sham, $n = 10$		P
Age (years)	21.80 (0.68)	21.00 (1.25)		0.14[c]
Sex (male/female)	7/8	6/4		0.51[b]
Education (years)	15.60 (1.06)	15.30 (1.06)		0.49[c]
BIS11	56.07 (6.23)	58.20 (6.30)		0.41[c]
AI	13.80 (2.18)	12.90 (2.28)		0.33[c]
MI	17.93 (3.01)	18.80 (3.08)		0.49[c]
NPI	24.33 (3.48)	26.50 (3.57)		0.14[c]

Notes: values are mean (standard deviation) or count
[a] One-way ANOVA. [b]Two-sided chi-squared test. [c]Two-sample t-test. rIFG = right inferior frontal gyrus, M1 = primary motor cortex, IP = in-phase, AP = anti-phase, BIS11 = Barratt Impulsiveness Scale Version 11, AI = Attentional Impulsiveness, MI = Motor Impulsiveness, NPI = Non-Planning Impulsiveness.

Fig. 3. Behavioural effect of IP rIFG-M1 stimulation in Experiment 1.
Within the rIFG-M1 IP, sham and rIFG-M1 AP groups, (**a**) SSRT change (post minus during) and (**b**) individual SSRT change (post minus during). SSRT = stop-signal reaction time. Error bars represent standard errors of the mean. $*p < 0.05$, two-way mixed-design analysis of variance.
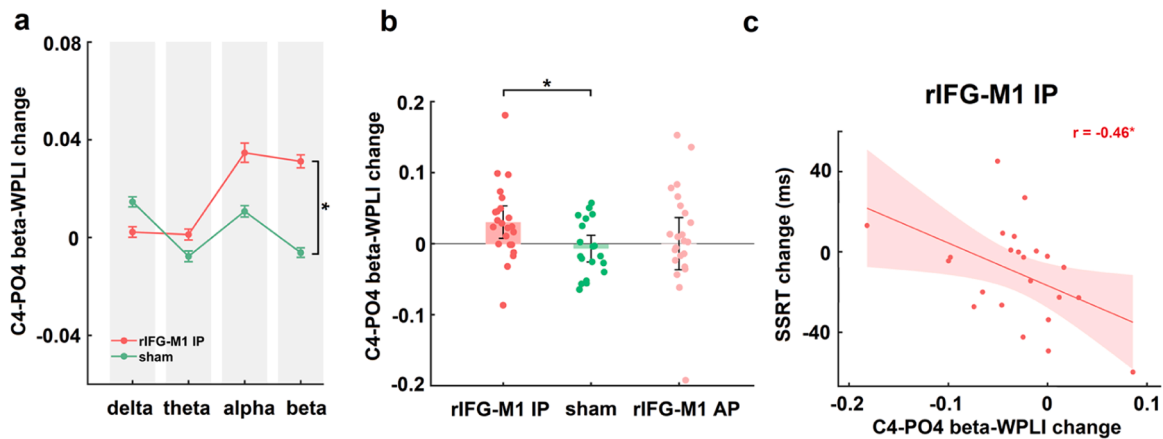
Fig. 4. Simulation-specific effects in Experiment 1.
(**a**) The line graph shows the changes (post minus pre) in WPLI across the four bands (delta, theta, alpha, and beta) of the rIFG-M1 IP and sham groups corresponding to the C4-PO4 pair. (**b**) Beta-WPLI changes (post minus pre) in the C4-PO4 pair in the rIFG-M1 IP, sham, and rIFG-M1AP groups. (**c**) The correlation between C4-PO4 beta-WPLI change and SSRT change in the rIFG-M1 IP group. $*p < 0.05$.
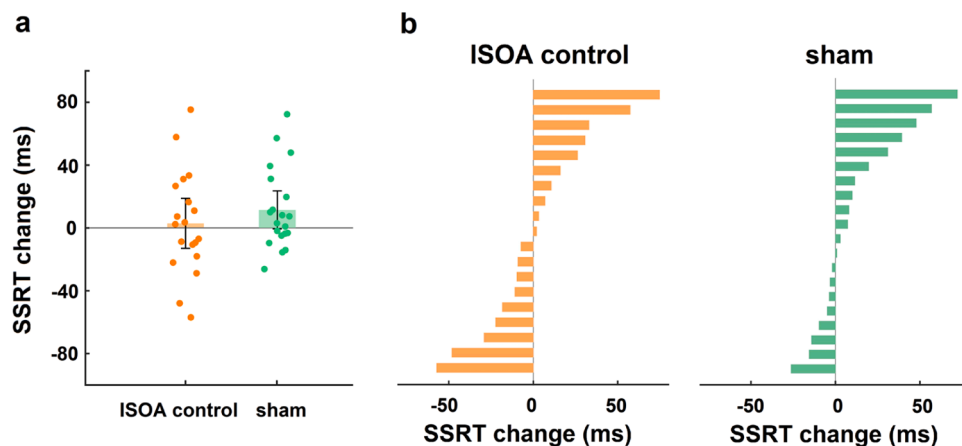
Fig. 5. Behavioural effect of the lSOA control group in Experiment 1.
Within the lSOA control group and sham groups, (**a**) SSRT change (post minus during) and (**b**) individual SSRT change (post minus during). lSOA = left supraorbital area. Error bars represent standard errors of the mean.

between the groups for blocks 2 to 4 relative to block 1. The two-sample *t*-test revealed that, compared to sham sessions, a significant reduction in SSRT was observed in the rIFG-M1 IP group only during the later period (block 3: $t_{68} = -3.68$, $p = 4.68\text{e-}04$, Cohen's $d = -0.89$; block 4:

$t_{68} = -3.23$, $p = 1.90\text{e-}03$, Cohen's $d = -0.78$, Fig. 7). These findings indicated that the impact of IP rIFG-M1 stimulation on response inhibition primarily occurs in the post-stimulation period.
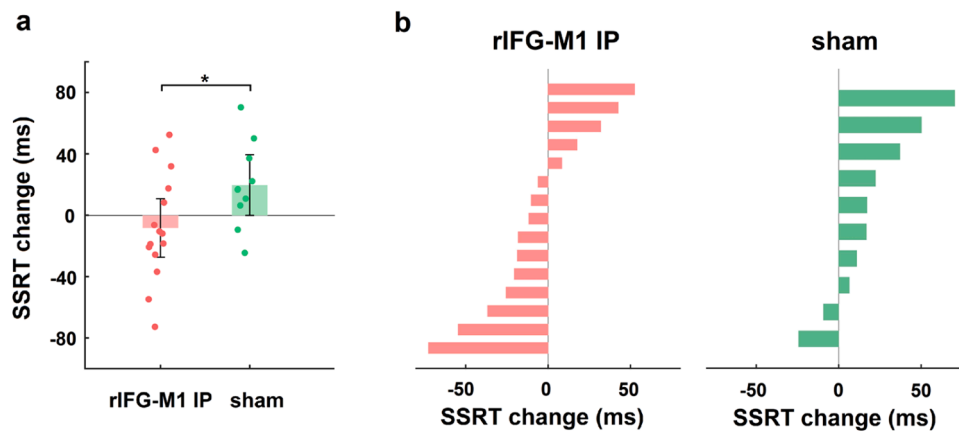
Fig. 6. Replication of SST improvements in the IP rIFG-M1 stimulation group in Experiment 2.
(**a**) SSRT change (post minus during) for rIFG-M1 IP and sham. (**b**): Individual SSRT change (post minus during) in the rIFG-M1 IP and sham groups. Error bars represent standard errors of the mean. *$p < 0.05$.
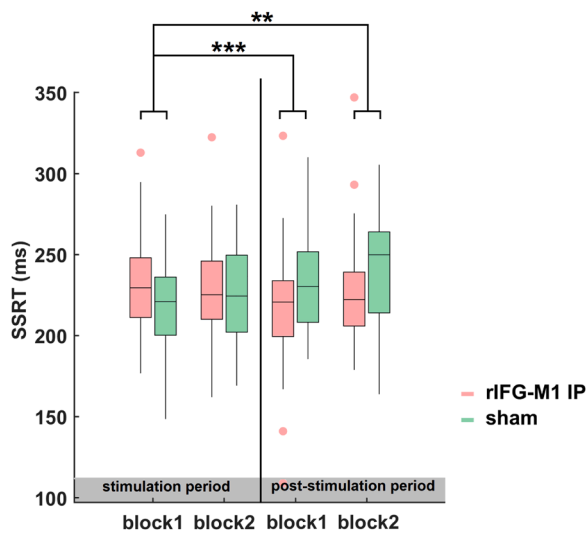
Fig. 7. Time dynamics of the behavioural results.
The boxplot shows the SSRT for blocks 1~4 (considering block 1 as the baseline) in the rIFG-M1 IP and sham groups in combined Experiments 1 and 2. *$p < 0.05$, **$p < 0.01$, ***$p < 0.001$, two-sample t-tests.

The state-dependence of SST improvements

In recent years, state-dependency has received considerable attention in the field of electrical stimulation research. Many studies have consistently reported that tACS interventions for cognition exhibit baseline state-dependency (Hu et al., 2022; Santarnecchi et al., 2016). Furthermore, we conducted an analysis using an external dataset from Liisa Raud et al.'s meta-analysis (Raud, Westerhausen, Dooley, & Huster, 2020) and found baseline state-dependency in response inhibition level (Supplementary Fig 4).

To explore the baseline state-dependent effects of dual-site tACS, we grouped the results based on the median SSRT (222.6 ms) of the stimulation period. Notably, participants with longer SSRT in the rIFG-M1 IP group showed decreased scores after stimulation (Fig. 8a), while the control group (rIFG-M1 AP and sham groups) did not (Fig. 8b). We further performed two-way mixed-design ANOVAs for the long SSRT and short SSRT groups. Within the long SSRT group, the analysis results revealed a significant group × time interaction effect among the rIFG-M1 IP, sham and rIFG-M1 AP groups ($F_{2,44} = 7.30$, $p = 1.83e-03$, $\eta_p^2 = 0.25$; Fig. 8c). Further analysis found that rIFG-M1 IP stimulation induced a significant decrease in the SSRT compared with sham

stimulation ($F_{1,33} = 11.68$, $p = 1.70e-03$, $\eta_p^2 = 0.26$; Fig. 8c). In contrast, rIFG-M1 AP stimulation did not significantly differ in SSRT from sham stimulation. In addition, rIFG-M1 IP stimulation induced a significant SSRT reduction compared with rIFG-M1 AP stimulation ($F_{1,31} = 9.37$, $p = 4.53e-03$, $\eta_p^2 = 0.23$; Fig. 8c). However, in the short SSRT group, there was no significant group × time interaction effect in the rIFG-M1 IP, sham and rIFG-M1 AP groups ($F_{2,44} = 1.86$, $p = 0.17$, $\eta_p^2 = 0.08$; Fig. 8d).

Given that participants with weaker response inhibition tend to exhibit higher impulsiveness (Eriksson, Jansson, Lisspers, & Sundin, 2016), we further investigated whether the improvements in response inhibition are state-dependent on baseline impulsiveness. A Pearson correlation analysis revealed a significant negative correlation between BIS11(AI) and SSRT changes in the rIFG-M1 IP group ($r = -0.53$, $p = 4.72e-04$, Fig. 8e). The results suggested greater improvement after stimulation in participants with higher AI, while no correlation was found in the control group (rIFG-M1 AP and sham groups) ($r = -0.18$, $p = 0.18$, Fig. 8f).

Together, our further exploration revealed the state dependence of response inhibition improvement, whereby response inhibition is enhanced in individuals with lower baseline response inhibition or higher impulsiveness.

Based on the median during-stimulation SSRT of the combined Experiments 1 and 2, those with higher or lower median SSRT were assigned to the long or short SSRT group, respectively. (**a**) Plot showing the SSRT during- and post-stimulation for the rIFG-M1 IP group, and (**b**) for the control group (rIFG-M1 AP and sham groups). The black circles show the distribution of long SSRTs. The histograms on the diagonal represent the frequency of the points under the corresponding position. (**c**) SST performance across three stimulation groups under the long SSRT condition and (**d**) under the short SSRT condition. (**e**) Correlations between BIS11 (Attentional Impulsiveness) and SSRT changes (post minus during) in the rIFG-M1 IP group and (**f**) in the control group (rIFG-M1 AP and sham groups) based on two experimental datasets. BIS11 = Barratt Impulsiveness Scale version 11, AI = Attentional Impulsiveness. Error bars represent standard errors of the mean. *$p < 0.05$, **$p < 0.01$, ***$p < 0.001$.

Discussion

We present evidence of improved response inhibition in healthy adults through IP dual-site beta-tACS over the rIFG-M1 network. Experiment 1 showed that IP beta-tACS over the rIFG-M1 network improved response inhibition and enhanced beta synchronization of the inhibitory control network, while AP beta-tACS did not. Furthermore, the increase in beta synchronization was significantly correlated with the improvement in response inhibition. The behavioural result was
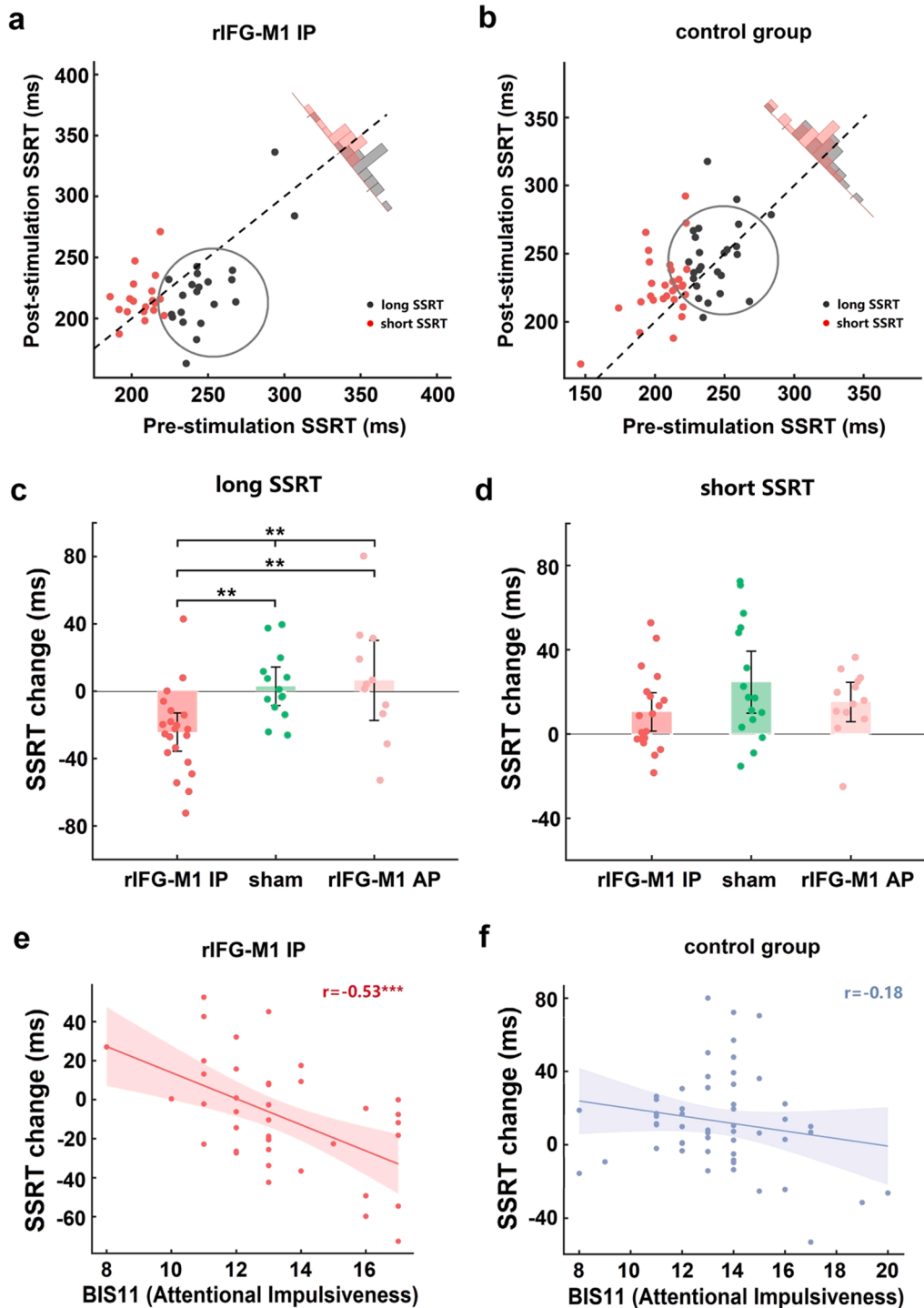
Fig. 8. The SST improvement was state-dependent on baseline cognitive control.

replicated in an independent sample of Experiment 2. Additionally, we observed that the behavioural effect occurred in the late post-stimulation period and was state-dependent on the individual baseline cognitive control level.

Improvements in response inhibition with IP dual-site beta-tACS

In the current study, we employed IP dual-site beta-tACS to modulate the rIFG-M1 network, which resulted in improved task performance. IP beta-tACS facilitated beta synchronization between the rIFG and M1, allowing for quick integration of attention-motion processing-related

control systems, which may work in the early stages of motion stopping, enabling motion to be stopped faster and subsequently resulting in increased response inhibition (Nakajima et al., 2022; Raud, Thunberg, & Huster, 2022; Raud et al., 2020; Schaum et al., 2021). Supporting this view, enhanced beta synchronization in the rIFG-M1 network and a positive association between increased network beta synchronization and improved response inhibition were also found in this study. Conversely, sham stimulation and AP beta-tACS over the rIFG-M1 network did not yield any positive effects on response inhibition or beta synchronization. These results suggested that beta synchronization within the rIFG-M1 network may serve as the foundation for stopping

motion. Furthermore, the effectiveness of IP rIFG-M1 stimulation may be attributed to the two-stage pause-then-cancel model proposed by a large body of recent and classical work in humans (Diesburg & Wessel, 2021; Tatz, Soh, & Wessel, 2021). By promoting quick attention and movement integration, IP beta-tACS modulation enables the rIFG-M1 network to minimize the early pause phase (Diesburg & Wessel, 2021; Raud et al., 2022, 2020).

The reproducibility of the IP rIFG-M1 stimulation effects in a new cohort of participants boosts the effect stability and confidence of the observed patterns. In Experiment 2, which was consistent with Experiment 1 in terms of experimental designs, IP rIFG-M1 stimulation showed significantly increased SST performance compared to the sham group. The reliability and replicability of the results obtained using repeated experiments with large samples and multiple control groups increases our confidence in concluding that the beta-synchronized rIFG-M1 network causally enhances individual response inhibition and eliminates the possibility that differences in brain state between groups of subjects lead to the main finding.

These results demonstrated that IP dual-site tACS can be used to modulate activity between cortical brain networks to enhance individual response inhibition, illustrating the plastic reorganization of potential brain networks by IP dual-site tACS. Phase synchronization may be beneficial in facilitating interregional oscillations to improve behaviour (Saturnino, Madsen, Siebner, & Thielscher, 2017), which could further support the view that network synchronization transmits information widely distributed in the brain to support behaviour (Alekseichuk et al., 2019; Polania, Moisa, Opitz, Grueschow, & Ruff, 2015). Furthermore, the results provide a possible explanation for the contradictory results of previous interventions in single cortical brain regions (Dambacher et al., 2015; Jacobson et al., 2011; Kwon et al., 2013; Thunberg et al., 2020; Yu, Tseng, Hung, Wu, & Juan, 2015). Dual-site tACS technology will also be a powerful tool for future causal analysis of cortical brain networks.

The temporal dynamic and state-dependent effect of dual-site tACS on response inhibition

We further refined our analysis by examining the specific temporal dynamics of SSRT during and after the stimulation period. Our results revealed that substantial changes in SSRT were observed exclusively after the completion of stimulation. This pattern of findings is consistent with previous investigations on tACS (Reinhart & Nguyen, 2019), which have consistently demonstrated that the observed enhancements in behaviour and electrophysiological measures occur in the post-stimulation phase rather than during the actual stimulation. This temporal dissociation between tACS application and its effects on cognitive processes may be attributed to the spike-time-dependent plasticity of synaptic activity. Synaptic events exhibit a certain degree of temporal delay, and their effects on neural processing are not immediately evident. Therefore, the effects of tACS are likely to manifest as delayed responses to stimulation, reflecting the complex temporal dynamics of synaptic modulation.

The state-dependent effects of tACS have been investigated in recent studies (Hu et al., 2022; Zanto et al., 2021). It has been shown that the interaction of tACS with cognitive tasks depends on the activation state of neurons in the target region. Moreover, we also identified the state-dependence of response inhibition through an analysis of data from Liisa Raud et al. (2022). In our study, we classified participants into long and short SSRT groups based on baseline median SSRT (Guo et al., 2022; Mattavelli et al., 2015). For IP rIFG-M1 stimulation, participants with long SSRTs were effective in improving task performance. However, in the short SSRT group, there was no significant improvement in all groups. We observed a greater tACS effect in the long SSRT group than in the short SSRT group, probably since better baseline response inhibition performance was associated with higher neural excitability, which is difficult to further enhance (Zanto et al., 2021). As shown by

previous neuroimaging studies, activation of inhibitory motor areas is negatively correlated with SSRT (Congdon et al., 2010; Tsvetanov et al., 2018), and there are individual differences in the neural mechanisms of inhibitory processing by the rIFG-M1 network.

Furthermore, studies have demonstrated that individuals with lower response inhibition exhibit higher attentional impulsiveness (Eriksson et al., 2016), and our observations indicated a relationship between the impact of IP rIFG-M1 stimulation on response inhibition and an individual's attentional impulsiveness. Specifically, we found that greater attentional impulsiveness was associated with more significant improvements in response inhibition. These findings suggest that participants' response inhibition improvements following IP rIFG-M1 stimulation were state-dependent on baseline attentional impulsiveness and that baseline attentional impulsiveness could predict the degree of response inhibition enhancement after IP rIFG-M1 stimulation.

As mentioned above, improvement of response inhibition by dual-site tACS is state-dependent on baseline cognitive control. Therefore, using new network approaches, such as dual-site tACS that was used in this paper, scientists can build brain-specific models of different individuals and help develop more effective clinically personalized treatment options (Thiebaut de Schotten & Forkel, 2022). Moreover, the findings may provide new clinical insights into the potential treatment effects of neurological disorders, such as attention deficit hyperactivity disorder, schizophrenia, or pathological gambling (Friehs, Frings, & Hartwigsen, 2021; Lawrence, Luty, Bogdan, Sahakian, & Clark, 2009; Lipszyc & Schachar, 2010; Weigard, Heathcote, Matzke, & Huang-Pollock, 2019).

Several limitations remained in the study. First, we provided evidence for enhanced response inhibition and functional connectivity of resting-state EEG under IP rIFG-M1 stimulation. Although resting-state EEG can be used to quantitatively study response inhibition mechanisms and most studies have used it for neural marker studies, resting-state EEG is difficult to integrate well with actual motor abilities (Khanna, Pascual-Leone, Michel, & Farzan, 2015) (Zebhauser, Hohn, & Ploner, 2022). Thus, we suggest that future research focus on deeper mechanisms using functional magnetic resonance imaging analysis of task states (Elliott et al., 2019; Krienen, Yeo, & Buckner, 2014). Second, we found an unbalanced electric field distribution in the tACS condition by electric field simulations due to the use of a common return electrode, where the left supraorbital area receives the sum of the currents applied simultaneously to the rIFG-M1 network. However, although IP dual-site tACS resulted in different electric field distributions in the brain, our results showed that the modulation of brain activity and synchronization were restricted only to cortical brain networks associated with response inhibition. Many studies have also found that the left supraorbital-located brain regions unrelated to response inhibition do not have a potential impact on stimulation effects (Ouellet et al., 2015). Meanwhile, we further excluded the stimulation effect of the "return" electrode by lSOA control stimulation. In addition, the area around the stimulating electrode showed weak stimulation responses. Future research could compare the stimulation effects of traditional dual-site tACS and high-definition tACS to achieve optimal stimulation outcomes. Finally, the current study only explored the immediate effect of IP rIFG-M1 stimulation to improve response inhibition, but no long-term effects have been followed up and investigated, which could be a research direction in which future studies find more effective interventions for patients with clinical response inhibition deficits.

Conclusion

In summary, we provide evidences that response inhibition works through the rIFG-M1 network by dual-site beta-tACS. This finding promotes a further understanding of the theoretical mechanisms of response inhibition and offers potential new treatment targets of synchronized cortical network activity for patients with clinically deficient response inhibition.

Financial disclosure statement

Materials & correspondence

Correspondence and requests for materials should be addressed to JB.

CRediT authorship contribution statement

Qiujian Meng: Data curation, Formal analysis, Methodology, Resources, Software, Validation, Visualization, Writing – original draft. **Ying Zhu:** Data curation, Formal analysis, Methodology, Resources, Software, Validation, Visualization, Writing – original draft. **Ye Yuan:** Methodology, Software, Validation. **Rui Ni:** Software, Validation, Writing – review & editing. **Li Yang:** Software, Validation, Writing – review & editing. **Jiafang Liu:** Software, Validation, Writing – review & editing. **Junjie Bu:** Conceptualization, Formal analysis, Funding acquisition, Investigation, Methodology, Project administration, Resources, Supervision, Writing – original draft.

Declaration of Competing Interest

The authors declare that they have no competing interests.

Supplementary materials

Supplementary material associated with this article can be found, in the online version, at doi:10.1016/j.ijchp.2023.100411.

References

Alderson, R. M., Rapport, M. D., & Kofler, M. J. (2007). Attention-deficit/hyperactivity disorder and behavioral inhibition: A meta-analytic review of the stop-signal paradigm. *Journal of Abnormal Child Psychology, 35*(5), 745–758. https://doi.org/10.1007/s10802-007-9131-6

Alekseichuk, I., Falchier, A. Y., Linn, G., Xu, T., Milham, M. P., Schroeder, C. E., & Opitz, A. (2019). Electric field dynamics in the brain during multi-electrode transcranial electric stimulation. *Nature Communications, 10*(1), 2573. https://doi.org/10.1038/s41467-019-10581-7

Aron, A. R., Robbins, T. W., & Poldrack, R. A. (2014). Inhibition and the right inferior frontal cortex: One decade on. *Trends in Cognitive Sciences, 18*(4), 177–185. https://doi.org/10.1016/j.tics.2013.12.003

Boehler, C. N., Appelbaum, L. G., Krebs, R. M., Hopf, J.-M., & Woldorff, M. G. J. N. (2010). Pinning down response inhibition in the brain—Conjunction analyses of the stop-signal task. *NeuroImage, 52*(4), 1621–1632. https://doi.org/10.1016/j.neuroimage.2010.04.276

Congdon, E., Mumford, J. A., Cohen, J. R., Galvan, A., Aron, A. R., Xue, G., … Poldrack, R. A. (2010). Engagement of large-scale networks is related to individual differences in inhibitory control. *NeuroImage, 53*(2), 653–663. https://doi.org/10.1016/j.neuroimage.2010.06.062

Congdon, E., Mumford, J. A., Cohen, J. R., Galvan, A., Canli, T., & Poldrack, R. A. (2012). Measurement and reliability of response inhibition. *Frontiers in Psychology, 3*, 37. https://doi.org/10.3389/fpsyg.2012.00037

Dambacher, F., Schuhmann, T., Lobbestael, J., Arntz, A., Brugman, S., & Sack, A. T. (2015). No effects of bilateral tDCS over inferior frontal gyrus on response inhibition and aggression. *PloS One, 10*(7), Article e0132170. https://doi.org/10.1371/journal.pone.0132170

Depue, B. E., Orr, J., Smolker, H., Naaz, F., & Banich, M. J. C. C. (2016). The organization of right prefrontal networks reveals common mechanisms of inhibitory regulation across cognitive, emotional, and motor processes. *Cerebral Cortex (New York, N.Y. : 1991), 26*(4), 1634–1646. https://doi.org/10.1093/cercor/bhu324

Diesburg, D. A., & Wessel, J. R. (2021). The Pause-then-Cancel model of human action-stopping: Theoretical considerations and empirical evidence. *Neuroscience and Biobehavioral Reviews, 129*, 17–34. https://doi.org/10.1016/j.neubiorev.2021.07.019

Elliott, M. L., Knodt, A. R., Cooke, M., Kim, M. J., Melzer, T. R., Keenan, R., … Hariri, A. R. (2019). General functional connectivity: Shared features of resting-state and task fMRI drive reliable and heritable individual differences in functional brain networks. *NeuroImage, 189*, 516–532. https://doi.org/10.1016/j.neuroimage.2019.01.068

Enz, N., Ruddy, K. L., Rueda-Delgado, L. M., & Whelan, R. (2021). Volume of β-bursts, but not their rate, predicts successful response inhibition. *The Journal of Neuroscience : The Official Journal of the Society For Neuroscience, 41*(23), 5069–5079. https://doi.org/10.1523/JNEUROSCI.2231-20.2021

Eriksson, L. J. K., Jansson, B., Lisspers, J., & Sundin, Ö. (2016). The interactive effect of the Behavioral Inhibition System (BIS) and response inhibition on accuracy in a modified stop-signal task. *Personality and Individual Differences, 97*, 198–202. https://doi.org/10.1016/j.paid.2016.03.057

Friehs, M. A., Frings, C., & Hartwigsen, G. (2021). Effects of single-session transcranial direct current stimulation on reactive response inhibition. *Neuroscience and Biobehavioral Reviews, 128*, 749–765. https://doi.org/10.1016/j.neubiorev.2021.07.013

Fries, P. (2015). Rhythms for Cognition: Communication through Coherence. *Neuron, 88*(1), 220–235. https://doi.org/10.1016/j.neuron.2015.09.034

Gordon, E. M., Chauvin, R. J., Van, A. N., Rajesh, A., Nielsen, A., Newbold, D. J., … Dosenbach, N. U. F. (2023). A somato-cognitive action network alternates with effector regions in motor cortex. *Nature, 617*(7960), 351–359. https://doi.org/10.1038/s41586-023-05964-2

Guo, Z., Gong, Y., Lu, H., Qiu, R., Wang, X., Zhu, X., & You, X. (2022). Multitarget high-definition transcranial direct current stimulation improves response inhibition more than single-target high-definition transcranial direct current stimulation in healthy participants. *Frontiers In Neuroscience, 16*, Article 905247. https://doi.org/10.3389/fnins.2022.905247

Helfrich, R. F., Knepper, H., Nolte, G., Strüber, D., Rach, S., Herrmann, C. S., … Engel, A. K. (2014). Selective modulation of interhemispheric functional connectivity by HD-tACS shapes perception. *PLoS Biology, 12*(12), Article e1002031. https://doi.org/10.1371/journal.pbio.1002031

Hogeveen, J., Grafman, J., Aboseria, M., David, A., Bikson, M., & Hauner, K. K. (2016). Effects of high-definition and conventional tDCS on response inhibition. *Brain Stimulation, 9*(5), 720–729. https://doi.org/10.1016/j.brs.2016.04.015

Hsu, T.-Y., Tseng, L.-Y., Yu, J.-X., Kuo, W.-J., Hung, D. L., Tzeng, O. J., … Juan, C.-H. J. N. (2011). Modulating inhibitory control with direct current stimulation of the superior medial frontal cortex. *NeuroImage, 56*(4), 2249–2257. https://doi.org/10.1016/j.neuroimage.2011.03.059

Hu, Z., Samuel, I. B. H., Meyyappan, S., Bo, K., Rana, C., & Ding, M. (2022). Aftereffects of frontoparietal theta tACS on verbal working memory: Behavioral and neurophysiological analysis. *IBRO Neuroscience Reports, 13*, 469–477. https://doi.org/10.1016/j.ibneur.2022.10.013

Jacobson, L., Javitt, D. C., & Lavidor, M. J. (2011). Activation of inhibition: Diminishing impulsive behavior by direct current stimulation over the inferior frontal gyrus. *Journal of Cognitive Neuroscience, 23*(11), 3380–3387. https://doi.org/10.1162/jocn_a_00020

Khanna, A., Pascual-Leone, A., Michel, C. M., & Farzan, F. (2015). Microstates in resting-state EEG: Current status and future directions. *Neuroscience and Biobehavioral Reviews, 49*, 105–113. https://doi.org/10.1016/j.neubiorev.2014.12.010

Krienen, F. M., Yeo, B. T. T., & Buckner, R. L. (2014). Reconfigurable task-dependent functional coupling modes cluster around a core functional architecture. *Philosophical Transactions of the Royal Society of London. Series B, Biological Sciences, 369*(1653). https://doi.org/10.1098/rstb.2013.0526

Kwon, J. W., Nam, S. H., Lee, N. K., Son, S. M., Choi, Y. W., & Kim, C. S. (2013). The effect of transcranial direct current stimulation on the motor suppression in stop-signal task. *NeuroRehabilitation, 32*(1), 191–196. https://doi.org/10.3233/NRE-130836

Kwon, Y. H., & Kwon, J. W. (2013a). Response inhibition induced in the stop-signal task by transcranial direct current stimulation of the pre-supplementary motor area and primary sensorimotor cortex. *Journal of Physical Therapy Science, 25*(9), 1083–1086. https://doi.org/10.1589/jpts.25.1083

Kwon, Y. H., & Kwon, J. W. (2013b). Is transcranial direct current stimulation a potential method for improving response inhibition? *Neural Regeneration Research, 8*(11), 1048. https://doi.org/10.3969/j.issn.1673-5374.2013.11.011

Lawrence, A. J., Luty, J., Bogdan, N. A., Sahakian, B. J., & Clark, L. (2009). Impulsivity and response inhibition in alcohol dependence and problem gambling. *Psychopharmacology, 207*(1), 163–172. https://doi.org/10.1007/s00213-009-1645-x

Leunissen, I., Van Steenkiste, M., Heise, K.-F., Monteiro, T. S., Dunovan, K., Mantini, D., … Swinnen, S. P. (2022). Effects of beta-band and gamma-band rhythmic stimulation on motor inhibition. *IScience, 25*(5), Article 104338. https://doi.org/10.1016/j.isci.2022.104338

Lipszyc, J., & Schachar, R. (2010). Inhibitory control and psychopathology: A meta-analysis of studies using the stop signal task. *Journal of the International Neuropsychological Society : JINS, 16*(6), 1064–1076. https://doi.org/10.1017/S1355617710000895

Logan, G. D. (1985). Executive control of thought and action. *Acta Psychologica, 60*(2–3), 193–210. https://doi.org/10.1016/0001-6918(85)90055-1

Logan, G. D. (2015). The point of no return: A fundamental limit on the ability to control thought and action. *Quarterly Journal of Experimental Psychology (2006), 68*(5), 833–857. https://doi.org/10.1080/17470218.2015.1008020

Mattavelli, G., Zuglian, P., Dabroi, E., Gaslini, G., Clerici, M., & Papagno, C. (2015). Transcranial magnetic stimulation of medial prefrontal cortex modulates implicit attitudes towards food. *Appetite, 89*, 70–76. https://doi.org/10.1016/j.appet.2015.01.014

Nakajima, K., Osada, T., Ogawa, A., Tanaka, M., Oka, S., Kamagata, K., … Konishi, S. (2022). A causal role of anterior prefrontal-putamen circuit for response inhibition revealed by transcranial ultrasound stimulation in humans. *Cell Reports, 40*(7), Article 111197. https://doi.org/10.1016/j.celrep.2022.111197

Ouellet, J., McGirr, A., Van den Eynde, F., Jollant, F., Lepage, M., & Berlim, M. T. J. (2015). Enhancing decision-making and cognitive impulse control with transcranial direct current stimulation (tDCS) applied over the orbitofrontal cortex (OFC): A randomized and sham-controlled exploratory study. *Journal of Psychiatric Research, 69*, 27–34. https://doi.org/10.1016/j.jpsychires.2015.07.018

Parkin, B. L., Hellyer, P. J., Leech, R., & Hampshire, A. (2015). Dynamic network mechanisms of relational integration. *The Journal of Neuroscience : The Official Journal of the Society For Neuroscience, 35*(20), 7660–7673. https://doi.org/10.1523/JNEUROSCI.4956-14.2015

Picazio, S., Veniero, D., Ponzo, V., Caltagirone, C., Gross, J., Thut, G., & Koch, G. (2014). Prefrontal control over motor cortex cycles at beta frequency during movement inhibition. *Current Biology : CB, 24*(24), 2940–2945. https://doi.org/10.1016/j.cub.2014.10.043

Polania, R., Moisa, M., Opitz, A., Grueschow, M., & Ruff, C. C. (2015). The precision of value-based choices depends causally on fronto-parietal phase coupling. *Nature Communications, 6*, 8090. https://doi.org/10.1038/ncomms9090

Polanía, R., Nitsche, M. A., Korman, C., Batsikadze, G., & Paulus, W. (2012). The importance of timing in segregated theta phase-coupling for cognitive performance. *Current Biology, 22*(14), 1314–1318. https://doi.org/10.1016/j.cub.2012.05.021

Rae, C. L., Hughes, L. E., Anderson, M. C., & Rowe, J. B. J. (2015). The prefrontal cortex achieves inhibitory control by facilitating subcortical motor pathway connectivity. *Journal of Neuroscience, 35*(2), 786–794.

Raud, L., Thunberg, C., & Huster, R. J. (2022). Partial response electromyography as a marker of action stopping. *eLife, 11*. https://doi.org/10.7554/eLife.70332

Raud, L., Westerhausen, R., Dooley, N., & Huster, R. J. (2020). Differences in unity: The go/no-go and stop signal tasks rely on different mechanisms. *NeuroImage, 210*, Article 116582. https://doi.org/10.1016/j.neuroimage.2020.116582

Reinhart, R. M. G., & Nguyen, J. A. (2019). Working memory revived in older adults by synchronizing rhythmic brain circuits. *Nature Neuroscience, 22*(5), 820–827. https://doi.org/10.1038/s41593-019-0371-x

Ridderinkhof, K. R., Van Den Wildenberg, W. P., Segalowitz, S. J., & Carter, C. S. (2004). Neurocognitive mechanisms of cognitive control: The role of prefrontal cortex in action selection, response inhibition, performance monitoring, and reward-based learning. *Brain and Cognition, 56*(2), 129–140. https://doi.org/10.1016/j.bandc.2004.09.016

Santarnecchi, E., Muller, T., Rossi, S., Sarkar, A., Polizzotto, N. R., Rossi, A., & Cohen Kadosh, R. (2016). Individual differences and specificity of prefrontal gamma frequency-tACS on fluid intelligence capabilities. *Cortex; a Journal Devoted To the Study of the Nervous System and Behavior, 75*, 33–43. https://doi.org/10.1016/j.cortex.2015.11.003

Saturnino, G. B., Madsen, K. H., Siebner, H. R., & Thielscher, A. (2017). How to target inter-regional phase synchronization with dual-site transcranial alternating current stimulation. *NeuroImage, 163*, 68–80. https://doi.org/10.1016/j.neuroimage.2017.09.024

Schaum, M., Pinzuti, E., Sebastian, A., Lieb, K., Fries, P., Mobascher, A., … Tüscher, O. (2021). Right inferior frontal gyrus implements motor inhibitory control via beta-band oscillations in humans. *eLife, 10*. https://doi.org/10.7554/eLife.61679

Stramaccia, D. F., Penolazzi, B., Sartori, G., Braga, M., Mondini, S., & Galfano, G. (2015). Assessing the effects of tDCS over a delayed response inhibition task by targeting the right inferior frontal gyrus and right dorsolateral prefrontal cortex. *Experimental Brain Research, 233*(8), 2283–2290. https://doi.org/10.1007/s00221-015-4297-6

Swann, N., Tandon, N., Canolty, R., Ellmore, T. M., McEvoy, L. K., Dreyer, S., … Aron, A. R. (2009). Intracranial EEG reveals a time-and frequency-specific role for the right inferior frontal gyrus and primary motor cortex in stopping initiated responses. *The Journal of Neuroscience : The Official Journal of the Society For Neuroscience, 29*(40), 12675–12685. https://doi.org/10.1523/JNEUROSCI.3359-09.2009

Tatz, J. R., Soh, C., & Wessel, J. R. (2021). Common and unique inhibitory control signatures of action-stopping and attentional capture suggest that actions are stopped in two stages. *The Journal of Neuroscience : The Official Journal of the Society For Neuroscience, 41*(42), 8826–8838. https://doi.org/10.1523/JNEUROSCI.1105-21.2021

Thiebaut de Schotten, M., & Forkel, S. J. (2022). The emergent properties of the connected brain. *Science (New York, N.Y.), 378*(6619), 505–510. https://doi.org/10.1126/science.abq2591

Thielscher, A., Antunes, A., & Saturnino, G. B. (2015). Field modeling for transcranial magnetic stimulation: A useful tool to understand the physiological effects of TMS?. In *Paper presented at the 2015 37th annual international conference of the IEEE engineering in medicine and biology society (EMBC)*.

Thunberg, C., Messel, M. S., Raud, L., & Huster, R. J. (2020). tDCS over the inferior frontal gyri and visual cortices did not improve response inhibition. *Scientific Reports, 10*(1), 1–10. https://doi.org/10.1038/s41598-020-62921-z

Tsvetanov, K. A., Ye, Z., Hughes, L., Samu, D., Treder, M. S., Wolpe, N., … Rowe, J. B. (2018). Activity and connectivity differences underlying inhibitory control across the adult life span. *The Journal of Neuroscience : The Official Journal of the Society For Neuroscience, 38*(36), 7887–7900. https://doi.org/10.1523/JNEUROSCI.2919-17.2018

Verbruggen, F., Aron, A. R., Band, G. P., Beste, C., Bissett, P. G., Brockett, A. T., … Colonius, H. J. (2019). A consensus guide to capturing the ability to inhibit actions and impulsive behaviors in the stop-signal task. *eLife, 8*, e46323. https://doi.org/10.7554/eLife.46323

Vinck, M., Oostenveld, R., van Wingerden, M., Battaglia, F., & Pennartz, C. M. A. (2011). An improved index of phase-synchronization for electrophysiological data in the presence of volume-conduction, noise and sample-size bias. *NeuroImage, 55*(4), 1548–1565. https://doi.org/10.1016/j.neuroimage.2011.01.055

Violante, I. R., Li, L. M., Carmichael, D. W., Lorenz, R., Leech, R., Hampshire, A., … Sharp, D. J. (2017). Externally induced frontoparietal synchronization modulates network dynamics and enhances working memory performance. *eLife, 6*, e22001. https://doi.org/10.7554/eLife.22001

Wagner, J., Wessel, J. R., Ghahremani, A., & Aron, A. R. (2018). Establishing a right frontal beta signature for stopping action in scalp EEG: Implications for testing inhibitory control in other task contexts. *Journal of Cognitive Neuroscience, 30*(1), 107–118. https://doi.org/10.1162/jocn_a_01183

Weigard, A., Heathcote, A., Matzke, D., & Huang-Pollock, C. (2019). Cognitive modeling suggests that attentional failures drive longer stop-signal reaction time estimates in attention deficit/hyperactivity disorder. *Clinical Psychological Science : A Journal of the Association For Psychological Science, 7*(4), 856–872. https://doi.org/10.1177/2167702619838466

Wessel, J. R. (2020). β-bursts reveal the trial-to-trial dynamics of movement initiation and cancellation. *The Journal of Neuroscience : The Official Journal of the Society For Neuroscience, 40*(2), 411–423. https://doi.org/10.1523/JNEUROSCI.1887-19.2019

Yu, J., Tseng, P., Hung, D. L., Wu, S. W., & Juan, C. H. (2015). Brain stimulation improves cognitive control by modulating medial-frontal activity and preSMA-vmPFC functional connectivity. *Human Brain Mapping, 36*(10), 4004–4015. https://doi.org/10.1002/hbm.22893

Zanto, T. P., Jones, K. T., Ostrand, A. E., Hsu, W.-Y., Campusano, R., & Gazzaley, A. (2021). Individual differences in neuroanatomy and neurophysiology predict effects of transcranial alternating current stimulation. *Brain Stimulation, 14*(5), 1317–1329. https://doi.org/10.1016/j.brs.2021.08.017

Zebhauser, P. T., Hohn, V. D., & Ploner, M. (2022). Resting state EEG and MEG as biomarkers of chronic pain: A systematic review. *Pain*. https://doi.org/10.1097/j.pain.0000000000002825